# Attosecond Transient Absorption Spectroscopy of doubly-excited states in helium

Luca Argenti[1],* Christian Ott[2], Thomas Pfeifer[2], and Fernando Martín[1,3]
[1] *Departamento de Química, Módulo 13, Universidad Autónoma de Madrid, 28049 Madrid, Spain, EU*
[2] *Max-Planck Institut für Kernphysik, Saupfercheckweg 1, 69117 Heidelberg, Germany*
[2] *Center for Quantum Dynamics, Ruprecht-Karls-Universität Heidelberg, 69120 Heidelberg, Germany and*
[3] *Instituto Madrileño de Estudios Avanzados en Nanociencia (IMDEA-Nanociencia), Cantoblanco, 28049 Madrid, Spain*
(Dated: November 13, 2012)

Strong-field manipulation of autoionizing states is a crucial aspect of electronic quantum control. Recent measurements of the attosecond transient absorption spectrum of helium dressed by a few-cycle visible pulse [Ott et al., arXiv:1205.0519[physics.atom-ph] ] provide evidence of novel ultrafast resonant phenomena, namely, two-photon Rabi oscillations between doubly-excited states and the inversion of Fano profiles. Here we present the results of accurate *ab-initio* calculations that agree with these observations and in addition predict that (i) inversion of Fano profiles is actually periodic in the coupling laser intensity and (ii) the supposedly dark $2p^2\ ^1$S state also appears in the spectrum. Closer inspection of the experimental data confirms the latter prediction.

PACS numbers: 31.15.ac, 32.80.Fb, 32.80.Rm, 32.80.Zb

The fast development of attosecond laser pulses in the last decade gave access to the time-resolved study of correlated electron dynamics in atoms, molecules and solids on their natural time scale [1]. In this context, attosecond transient absorption spectroscopy (ATAS) [2] is emerging as a prominent technique complementary to the technologies which detect charged photofragments, like COLTRIMS [3] and VMI [4], to monitor and control transiently bound states. Compared to photofragment detection, ATAS provides higher energy resolution, and is applicable to condensed phases [5] as well as to the gas phase, thus making it a good candidate for the investigation of ultrafast electron dynamics in chemically relevant samples. Moreover, on the theoretical side, ATA spectra are significantly less demanding to reproduce than photoelectron distributions. While the latter require specification of scattering boundary conditions, the former only need the electronic wave function in the vicinity of the reaction center.

So far, ATAS has been employed to track both field-free ultrafast dynamics of coherent ensembles of valence-hole excited states [2, 6], as well as the driven dynamics induced by strong external visible (VIS) or near-infrared (NIR) dressing fields [7–12], including the following processes: electromagnetically induced transparency (EIT) [9, 10]; instantaneous ac-Stark shift [8]; multiphoton transition matrix elements [12]; interference of wavepackets [11]; and time-resolved autoionization [7].

In a recent experiment [9], ATAS has been used to investigate helium under the influence of a VIS dressing field at tunable intensity in the energy region of the doubly-excited states converging to the N=2 threshold. The experiment revealed clear Autler–Townes splitting of the $2s2p$ autoionizing state (the lowest term in the $sp^+_{2,2}\ ^1$P$^o$ bright series) due to the coupling between this state, the $2p^2\ ^1$S state, and the consecutive $sp^+_{2,3}$ state, and inversion of the characteristic Fano profile asymmetry in the higher terms of the $sp^+_{2,n}$ series as a function of both the pump-probe time delay and of the intensity of the VIS dressing field.

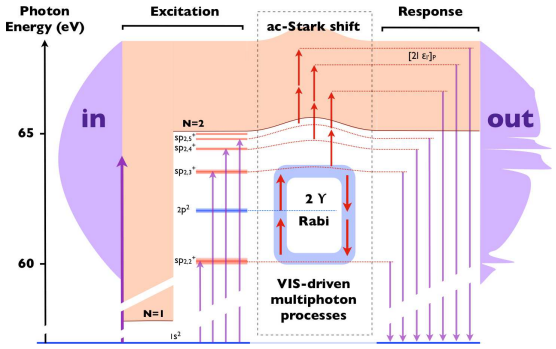


FIG. 1. **Energy level scheme.** The attosecond transient absorption spectrum of helium records the linear response of the atom, dressed by a strong external VIS field, in the extreme ultraviolet (XUV) energy range. A sub-femtosecond broadband XUV pulse excites a wide range of states in the single-ionization region. The population and phase of the states so created is altered as a result of the interaction with the strong dressing field, due to multiphoton or even non-perturbative transitions. The XUV dipole response of the atom reflects such composition changes.

Here we present the results of accurate *ab-initio* calculations that reproduce the experimental conditions in [9]. We compute the TAS of a sub-femtosecond extreme ultraviolet (XUV) pulse for a helium atom dressed by a short (7 fs) visible laser pulse (730 nm), as a function of the time delay between the two pulses and of the peak intensity of the dressing field. Our calculations are in excellent agreement with most of the current experimental results and point towards further interesting quantum phenomena of the physics of two interacting electrons exposed to both the Coulomb field of the nucleus and a laser field. In particular, the inversion of Fano profiles

is actually found to be periodic in the laser intensity, in agreement with the interpretation of this effect in terms of the energy shift of the doubly-excited states, which is approximately proportional to the intensity of the dressing laser [9]. Moreover, clear signatures of the supposedly dark $2p^2\ ^1$S state are observed. Finally, we show that the ATA spectrum can be construed in terms of the non-diagonal component of the linear electrical susceptibility of the dressed atom.

In the ATAS experiment under examination, the weak 60 eV XUV pulse $\mathcal{E}(t)$ induces a time-dependent dipole moment $d(t;\mathcal{E})$ in the atom dressed by the VIS field, which in turn results in a dipole emission that coherently contributes to the XUV field, thus altering its spectrum (see Fig. 1). For an optically thin medium, the relative change of the spectral intensity of the XUV pulse can be expressed in terms of an effective transient absorption atomic cross section $\sigma(\omega;\tilde{\mathcal{E}})$ [13]

$$\sigma(\omega;\tilde{\mathcal{E}}) = \frac{4\pi\omega}{c}\,\Im m\frac{\tilde{d}(\omega;\tilde{\mathcal{E}})}{\tilde{\mathcal{E}}(\omega)} \qquad (1)$$

where $\tilde{d}$ and $\tilde{\mathcal{E}}$ are the Fourier transform of the component of the dipole moment and the XUV field along the laser polarization, respectively, and where we emphasize the functional dependence of the response on the full spectrum of the impinging attosecond pulse. In this process, strongly correlated doubly-excited states (DES) have a preponderant role. For the latter, common models to evaluate the rate of non-perturbative processes, like ionization by tunneling [14, 15], are inapplicable, due to the complete breakdown of the single-active-electron (SAE), the adiabatic, and the non-polarizable parent-ion approximations [16, 17]. In this context, calculations based on simplified models [8, 18–24], SAE, or stationary methods, like Floquet theory [13, 25] have therefore limited applicability. The interpretation of these experiments require instead both a complete *ab-initio* representation of the system and a direct solution of the time-dependent Schrödinger equation (TDSE).

Here, we solve the TDSE with a Krylov representation of a second-order exponential unitary time-step propagator in velocity gauge [26]. Reflection from the box boundaries is prevented by complex absorbing potentials. The wave function is expanded on a two-particle spherical basis, the angular part is represented by bipolar spherical harmonics [27] and the radial part by B-splines with an asymptotic spacing of 0.5 au. Each total angular momentum comprises all the partial-wave channels with configurations of the form $N\ell\epsilon_{\ell'}$ with $N \leq 2$, and a full-CI localized channel $n\ell n'\ell'$ that reproduces short-range correlations between the two electrons [28]. Such representations of the correlated electron basis is able to represent in a concise way and with high accuracy all the resonant series in helium converging to any given threshold $N$ [28],and, thanks to the localized channel, the first few doubly-excited states converging to thresholds not included in the close-coupling expansion as well. The ATAS response is evaluated with a velocity-gauge analogue of (1), obtained via an application of the Ehrenfest theorem

$$\sigma(\omega;\tilde{\mathcal{E}}) = -\frac{4\pi}{\omega}\,\Im m\,\frac{\tilde{p}(\omega;\tilde{A})}{\tilde{A}(\omega)}, \qquad (2)$$

where $\tilde{A}$ and $\tilde{p}$ are the FT of the vector potential and the canonical momentum. The momentum $\tilde{p}$ is given by the sum of two complementary terms: $\tilde{p}_-$, computed numerically while in the presence of the dressing field, and $\tilde{p}_+$, computed analytically for the subsequent field-free evolution. The result is thus equivalent to the one that would be obtained for a simulation protracted for an infinite time. In the simulation, we include the states with orbital angular momentum up to $\ell_{max} = 5$ for the localized channel, and a total angular momentum up to $L_{max} = 10$. We checked for convergence with respect to both these limits by repeating few calculations with either $L_{max} = 15$ or $\ell_{max} = 10$, as well as by including the $N = 3$ partial-wave channels, without observing any significant change in the result.

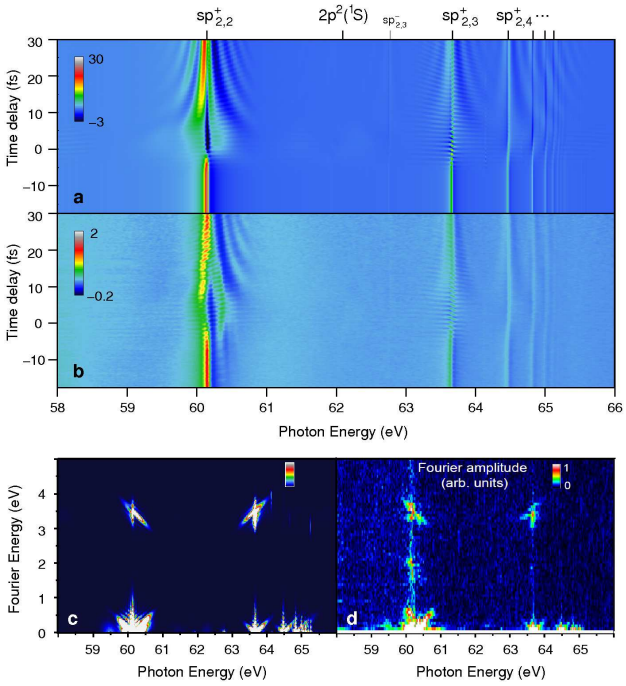


FIG. 2. ATAS as a function of the time delay. a) Theoretical transient absorption spectrum as a function of the XUV photon energy (x-axis) and of the time delay (y-axis) between the XUV and the VIS pulses, for a VIS intensity I=3.5 TW/cm$^2$. b) Matching experimental spectrum recorded for a nominal VIS intensity of 2.5±1.5 TW/cm$^2$. c) Theoretical, d) Experimental Fourier transform with respect to the time delay of the spectra shown in panel a-b).

In Fig. 2-a,b we compare the present theoretical ATAS spectrum $\sigma(\omega;\tau)$, as a function of the photon energy

and the time delay $\tau$, to the experimental optical density (OD) [9] (OD $\propto \sigma$). The agreement is excellent. The vertical features visible in the two spectra are due to the bright $sp^+_{2,n}$ series of doubly-excited states, $n = 2, 3, \ldots$ [29]. At large negative time delays, when the dressing pulse comes well before the XUV pulse, the ATAS spectrum displays the characteristic Fano profiles [29–31] of the field-free atom. When the two pulses overlap, the $sp^+_{2,2}$ state separates in two branches; this is the well known [9, 19, 23] Autler–Townes splitting (ATS) associated with the strong coupling between the $sp^+_{2,2}$ and the $2p^2\ ^1$S state, which, with the current energy of the dressing field, 1.7 eV, is resonantly coupled to both the first and the second term of the $sp^+_{2,n}$ series (see Fig. 1). The faint transversal wavelike features visible around both the $sp^+_{2,2}$ and the $sp^+_{2,3}$ terms for positive time delays are slices of the hyperbolic branches $\tau_n(E) = 2\pi n/|E - E_0|$. These features are caused by the beating between the amplitude of the resonantly-enhanced two-photon transition from one XUV-excited autoionizing state to the continuum-coupled other resonant state and the amplitude of the XUV transition from the ground state to the same coupled-resonant and continuum states. As far as the direct-ionization part is concerned, such phenomenon is the transient-absorption analogue to the one described for the photoelectron spectrum in [32]. At very large time delays, the signal converges again to the field-free case. Here, the fringes converging around each resonance are a consequence of the sharp change in the phase or population of the localized part of the resonances induced by the strong VIS pulse. Finally, in the dark narrow region between the two Autler–Townes branches of the $sp^+_{2,2}$ state the effective transient absorption cross section is *negative*, what indicates that the XUV field in that region is actually amplified rather than absorbed, as a result of the interaction with the atom. This observation confirms previous predictions [13, 23, 33] and experimental findings [6].

In Fig. 2-c,d we compare the FT with respect to the time delay of the ATA spectra in Fig. 2-a,b [34]

$$\tilde{\sigma}(\omega, \omega_\tau) = \int_{-\infty}^{\infty} d\tau \, \frac{e^{-i\omega_\tau \tau}}{\sqrt{2\pi}} \left[\sigma(\omega, \tau) - \sigma(\omega, \infty)\right], \qquad (3)$$

where $\omega_\tau$ is the Fourier Energy. To interpret such bi-dimensional spectra, let us consider again Eq. 1. Since the XUV pulse is weak, the dipole response of the laser-driven system can be assumed to be linear

$$\tilde{d}(\omega; \mathcal{E}) = \int d\omega' \chi(\omega, \omega') \tilde{\mathcal{E}}(\omega'). \qquad (4)$$

where $\chi(\omega, \omega')$ is the electric susceptibility of the dressed atom. For time-invariant samples, of course, the susceptibility is diagonal: $\chi(\omega, \omega') = \delta(\omega - \omega')\chi_d(\omega)$. This is not the case here, however. Under the action of any given excitation frequency, a dressed atom will in general

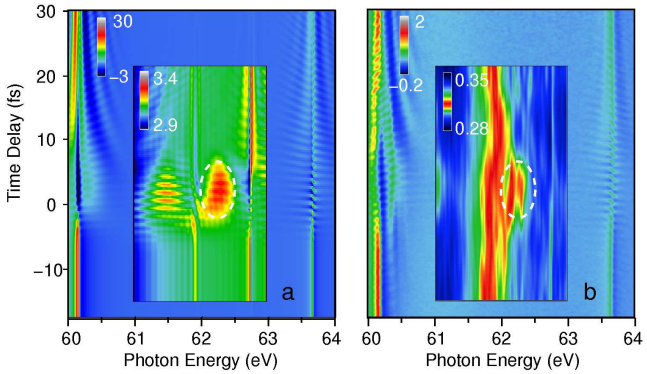


FIG. 3. Detail of the comparison between theoretical (left panel) and experimental (right panel) ATAS as a function of the XUV photon energy (x-axis) and of the time delay between VIS and XUV pulses (y-axis) in the energy region between the $sp^+_{2,2}$ and the $sp^+_{2,3}$ doubly-excited states. In the insets, closer inspection unveils a clear signature of the $2p^2\ ^1$S resonance, which mediates the transition between the lowest $^1$P bright states.

give rise to a response at other frequencies as well. This means that, alongside the field-free diagonal component, the electrical susceptibility also comprises a non-diagonal component $\chi_{nd}$,

$$\chi(\omega, \omega') = \delta(\omega - \omega')\chi_d(\omega) + \chi_{nd}(\omega, \omega'). \qquad (5)$$

For moderate intensities of the dressing lasers, the strongest features of $\chi_{nd}$ are expected to be located close to the diagonals $\omega = \omega' \pm 2n\omega_{vis}$. If the spectrum of the exciting laser is narrower than $2\omega_{vis}$, as in [13, 35, 36], transient absorption spectroscopy only probes the response close to the central diagonal $\omega = \omega'$. This provides valuable yet incomplete information on the ultrafast optical response of the dressed system. In the present ATAS, on the other hand, the spectral width of attosecond pulse exceeds $2\omega_{vis}$, therefore the response at $\omega = \omega' \pm 2\omega_{vis}$ results in a detectable heterodyne signal. This result holds for isolated as well as for trains [10–12] of attosecond pulses. The variation of the XUV field due to the change in time delay $\tau$ with respect to the dressing field, which defines the time origin, is readily parametrized as

$$\tilde{\mathcal{E}}(\omega) = \tilde{\mathcal{E}}(\omega; \tau) = e^{-i\omega\tau} \tilde{\mathcal{E}}_0(\omega), \qquad (6)$$

where $\tilde{\mathcal{E}}_0$ corresponds to a pulse centered at the time origin. From Eqns. (1-6) and in the limit of extremely short single pulses, where $\tilde{\mathcal{E}}_0(\omega)$ is eventually constant in an interval of the order of the excitation frequencies of the system, we obtain

$$\frac{ic\ \tilde{\sigma}(\omega, \omega_\tau)}{(2\pi)^{3/2}\omega} \simeq \chi_{nd}(\omega, \omega - \omega_\tau) - \chi^*_{nd}(\omega, \omega + \omega_\tau) \qquad (7)$$

The strong signals close to the $\omega_\tau = 0$ axis, therefore, are associated to the electromagnetically induced trans-

parency (EIT) of the DES that is visible also in femtosecond TAS [13, 20, 24]. The two strong features above the $sp^+_{2,2}$ and the $sp^+_{2,3}$ resonances at $\omega_\tau = 2\omega_{vis} = 3.4$ eV, instead, are heterodyne signals that are visible only in ATAS. In particular, the one above the $sp^+_{2,2}$ state can be assigned to the $\chi^*_{nd}(\omega_{sp^+_{2,3}} - 2\omega_{vis}, \omega_{sp^+_{2,3}})$ component of $\tilde{\sigma}$, while the one above the $sp^+_{2,3}$ state to the $\chi_{nd}(\omega_{sp^+_{2,2}} + 2\omega_{vis}, \omega_{sp^+_{2,2}})$ component. Both signals are strongly enhanced by the presence of the resonant $2p^2\ ^1$S intermediate state (compared to the higher terms in the $sp^+_{2,n}$ series) and comprise a non-resonant as well as a resonant part. The latter is indicative of an incipient resonant two-photon Rabi oscillation between the two $^1$P$^o$ states (see Fig. 1).

As a consequence of its even parity, the $2p^2\ ^1$S is normally a "dark" state. Yet, due to the effect of the dressing field both on it and on the ground state, the dipole amplitude between these two states is not exactly zero. Indeed, two faint signals at photon energy $\sim$ 61.5 eV and $\sim$ 62.3 eV close to the $\omega_\tau = 0$ axis are visible in Fig. 2. To confirm this observation, in figure 3 we show the theoretical and experimental ATAS with enhanced-contrast insets close to where the $2p^2\ ^1$S is expected to emerge. The upper Autler-Townes branch of this state is clearly visible in both insets with an intensity comparable to that of the narrow $sp^-_{2,3}\ ^1$P$^o$ resonance. This result shows that TAS is not restricted to the study of bright states only. Also "dark" states which are coupled to bright ones can emerge.

Fig. 4a shows the experimental ATAS for overlapping XUV and VIS pulses, as a function of the intensity of the dressing laser. The spectrum is averaged over a time-delay window of 1.2 fs to reduce the noise. Fig. 4bc show the theoretical prediction for a fixed time delay $\tau = 200$ au (maximum ATS). Overall, except for the highest intensities, the agreement is good: we observe the increase of the ATS of the $sp^+_{2,2}$ resonance as well as the inversion of the asymmetry of the Fano profile for all the higher terms in the $sp^+_{2,n}$ series as the intensity of the dressing field increases. In [9], this latter effect has been attributed to the ac-Stark shift $\Delta E_{ac-Stark}(t)$ of the localized component autoionizing states. The energy shift translates into an extra phase $\Delta\phi(\tau) = -\int_\tau^\infty \Delta E_{ac-Stark}(t')dt'$ between resonant and background amplitude that is approximately proportional to the peak intensity of the laser. As a consequence, the asymmetry (Fano profile) inversion is expected to be periodic in the laser intensity. Our calculations (see Fig. 4) clearly confirm this behavior. In the experimental spectrum, all resonant features suddenly fade for intensities larger than 4 TW/cm$^2$, close to the instrumental limit, which is sufficient to observe just the first inversion for the highest terms in the series. Convolution of the theoretical results in Fig. 4c with the experimental energy and intensity resolutions ($\sigma_E \simeq$20 meV and

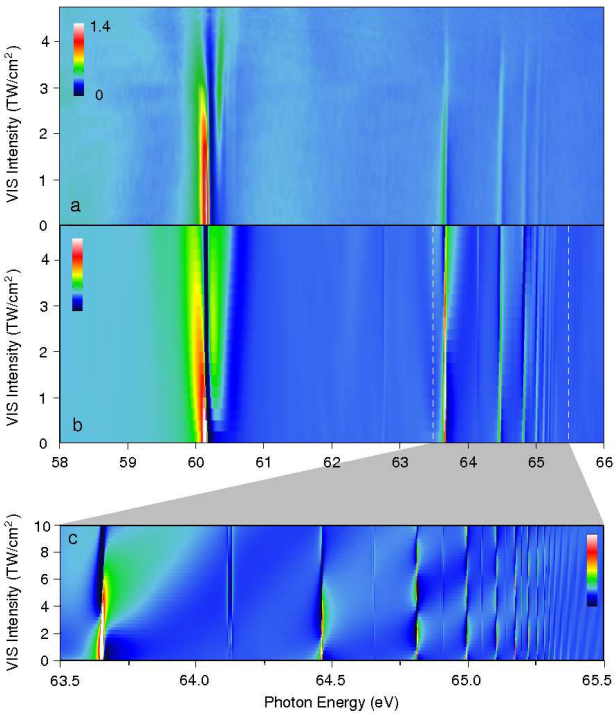


FIG. 4. ATAS for overlapping XUV and VIS pulses as a function of the XUV photon energy (x-axis) and of the intensity of the VIS dressing field (y-axis): a) experimental results (OD); b) theoretical prediction; c) detail of the theoretical prediction (notice the extended intensity range). The experimental and theoretical results are in good qualitative agreement at low intensities. While the experimental signal seems to fade at I=4TW/cm$^2$, the calculations predict ongoing resonant features up to intensities as high as 10 TW/cm$^2$. In particular, the characteristic flip in the asymmetry of the resonant Fano profiles doesn't occur just once, as observed in the experiment; instead, it is periodic in the intensity of the dressing field. See text for more details.

$\sigma_I \simeq 20\%\, I$, respectively) is found to smear out the resonant features at intensities higher than 5 TW/cm$^2$. The ac-Stark shift of singly-excited states in helium are known to approach the ponderomotive energy [25], which is the limiting value expected for a Rydberg electron bound to an unpolarizable core [37]. For the highest terms of the autoionizing $sp^+_{2,n}$ series, instead, our calculations show that the ac-Stark shift is significantly larger than such limit. In fact, in DES the two electrons are strongly correlated: for the higher terms in the $sp^+_{2,n}$ series, e.g., the parent ion is permanently polarized towards the outer electron. This is further indication that traditional formulas for estimating polarizability, tunneling rates and ac-Stark shifts are inapplicable to DES. At higher intensities, not shown here, we observe a multi-branch splitting of the $sp^+_{2,2}$ doubly-excited state that we associate to the multi-photon Rabi oscillation between the $sp^+_{2,2}$, the $2p^2\ ^1$S and the $sp^+_{2,3}$ states.

Some simplifying assumptions in the calculations are

likely responsible for the occasional discrepancies between theory and experiment. In particular, the theoretical XUV pulse has a purely Gaussian spectrum, while the experimental spectrum shows some residual odd-harmonic modulation. Furthermore, we do not represent the wide pedestal that is known to accompany the main VIS dressing pulse in practice. Finally, we didn't take advantage of the systematic relative uncertainty, of the order of ±20%, introduced by the calibration of the VIS intensity absolute value. Even so, the remarkable agreement with either the data recorded at the nominal intensity of 3.5 TW/cm$^2$ reported in [9] and those used in the present work is evidence that our conclusions are robust and sound.

In conclusion, in this work we showed how the inversion of asymmetric resonant transient absorption profiles in ATAS of dressed helium is periodic in the intensity of the driving laser, and that the field-free dark $2p^2\ ^1$S state actually gives rise to a distinct signal in the ATA spectrum under the influence of a moderately strong VIS laser field. The relation of TAS spectra to the non-diagonal component of the electrical susceptibility highlighted in this work offers an alternative and rational perspective on ATAS spectroscopy and suggests a direct way to measure and thus modulate the ac-Stark shift in transiently bound states, which is an important tool for the implementation of quantum-control protocols. Finally, the observation that the ac-Stark shift of autoionizing states close to the N=2 threshold is larger than the theoretical limit in the single-active electron approximation is an indication that common model tunneling-rate formulas are inapplicable to such states and, by extension, to any multi-electron atom where polarization of the core affects the effective field strength experienced by the ionizing active electron.

We thank Eva Lindroth for useful discussions during the early stages of this investigation. We thank Mare Nostrum BSC and CCC-UAM (Centro de Computación Científica, Universidad Autónoma de Madrid) for allocation of computer time. The research leading to these results has received funding from the European Research Council under the European Union's Seventh Framework Programme (FP7/2007-2013)/ERC grant agreement n290853, the European COST Action CM0702, the ERA-Chemistry project n° PIM2010EEC-00751, the Marie Curie ITN CORINF, the MICINN project n° FIS2010-15127, ACI2008-0777 and CSD 2007-00010 (Spain). CO and TP acknowledge financial support by the Max-Planck Research Group Program of the Max-Planck Gesellschaft (MPG).

* luca.argenti@uam.es

[1] F. Krausz and M. Y. Ivanov, Rev. Mod. Phys. **81**, 163 (2009).
[2] E. Goulielmakis *et al.*, Nature **466**, 739 (2010).
[3] J. Ullrich *et al.*, Rep. Prog. Phys. **66**, 1463 (2003).
[4] A. T. J. B. Eppink and D. H. Parker, Rev. Sci. Instrum. **68**, 3477 (1997).
[5] T. Pfeifer *et al.*, Chem. Phys. Lett. **463**, 11 (2008).
[6] A. Wirth *et al.*, Science **334**, 195 (2011).
[7] H. Wang *et al.*, Phys. Rev. Lett. **105**, 143002 (2010).
[8] M. Chini *et al.*, Phys. Rev. Lett. **109**, 073601 (2012).
[9] C. Ott *et al.*, arXiv [physics.atom-ph] **05**, 0519v1 (2012).
[10] P. Ranitovic *et al.*, Phys. Rev. Lett. **106**, 193008 (2011).
[11] M. Holler, F. Schapper, L. Gallmann, and U. Keller, Phys. Rev. Lett. **106**, 123601 (2011).
[12] N. Shivaram, H. Timmers, X.-M. Tong, and A. Sandhu, Phys. Rev. Lett. **108**, 193002 (2012).
[13] M. Gaarde, C. Buth, J. Tate, and K. Schafer, Phys. Rev. A **83**, 013419 (2011).
[14] M. V. Ammosov, N. B. Delone, and V. P. Krainov, JETP **91**, 2008 (1986).
[15] A. M. Perelomov, V. S. Popov, and M. V. Terent'ev, Sov. Phys. JETP **23**, 924 (1966).
[16] M. Smits, C. de Lange, A. Stolow, and D. Rayner, Physical Review Letters **93**, 1 (2004); **93**, 19 (2004).
[17] A. N. Pfeiffer *et al.*, arXiv (2011).
[18] P. Lambropoulos and P. Zoller, Phys. Rev. A **24**, 379 (1981).
[19] H. Bachau, P. Lambropoulos, and R. Shakeshaft, Phys. Rev. A **34**, 4785 (1986).
[20] Z.-H. Loh, C. H. Greene, and S. R. Leone, Chem. Phys. **350**, 7 (2008).
[21] S. I. Themelis, P. Lambropoulos, and M. Meyer, J. Phys. B: At. Mol. Opt. Phys. **37**, 4281 (2004).
[22] W.-c. Chu, S.-f. Zhao, and C. Lin, Phys. Rev. A **84**, 033426 (2011).
[23] W.-C. Chu and C. D. Lin, Phys. Rev. A **85**, 013409 (2012).
[24] W.-C. Chu and C. D. Lin, arXiv [physics.atom-ph] **05**, 5 (2012).
[25] X. M. Tong and N. Toshima, Phys. Rev. A **81**, 063403 (2010).
[26] L. Argenti and E. Lindroth, Phys. Rev. Lett. **105**, 053002 (2010).
[27] D. A. Varshalovich, A. N. Moskalev, and V. K. Khersonskii, *Quantum Theory of Angular Momemtum* (World Scientific Publishing, Singapore, 1988), p. 514.
[28] L. Argenti and R. Moccia, J. Phys. B: At. Mol. Opt. Phys. **39**, 2773 (2006); **41**, 035002 (2008); L. Argenti, At. Data. Nucl. Data Tables **94**, 903 (2008).
[29] J. W. Cooper, U. Fano, and F. Prats, Phys. Rev. Lett. **10**, 518 (1963).
[30] U. Fano, Phys. Rev. **124**, 1866 (1961).
[31] R. P. Madden and K. Codling, Phys. Rev. Lett. **10**, 516 (1963).
[32] J. Mauritsson *et al.*, Phys. Rev. Lett. **105**, 053001 (2010).
[33] F. Schapper *et al.*, Int. Conf. Ultrafast Phenom., ThA3 (2010).
[34] For the sake of clarity, we have removed the spectral asymptote $\sigma(\omega,\infty)$, which corresponds to the optical response of the field-free atom.
[35] C. Buth, R. Santra, and L. Young, Physical Review Letters **98**, 2 (2007).
[36] C. Buth and R. Santra, Physical Review A **78**, 1 (2008).
[37] M. D. Davidson, J. Wals, H. G. Muller, and H. B. van Linden van den Heuvell, Phys. Rev. Lett. **71**, 2192 (1993).